Results in Engineering 11 (2021) 100244

Contents lists available at ScienceDirect

Results in Engineering

journal homepage: www.sciencedirect.com/journal/results-in-engineering

On the design of a wheel assembly for a race car

Greg Wheatley [a,*], Mohammad Zaeimi [b]

[a] College of Science and Engineering, James Cook University, Townsville, Australia
[b] Mechanical Engineering Department, University of Guilan, Rasht, Iran

ARTICLE INFO

Keywords:
Wheel assembly
Upright
Brake rotor
Hub shaft
Formula SAE

ABSTRACT

Formula SAE (FSAE) is a competition where university students are challenged to design, fabricate and race small open-wheeled vehicles. This work outlines the development and analysis of a wheel assembly for a race car which carried out by the James Cook University Motorsports. A number of strategies are utilized throughout the paper including load calculations, modelling by SolidWorks and finite element analysis via Ansys for each part of the system including the upright, braking system and hub shaft.

1. Introduction

The wheel assembly is an integral part of a Formula SAE (FSAE) car and consists of several components such as the upright, braking system, hub shaft and wheel. Each component must be designed to account for factors that will affect the entire assembly and its function. These include: unsprung mass, camber, Ackermann steering geometry and brake fade.

The upright is a major component to the wheel assembly as its function is to provide a connection between the suspension and wheel, plus a mounting point for the brake calliper. It is constantly in motion with the wheel and is a load-bearing part of the suspension system. To optimize performance in a FSAE competition, it is imperative the upright is lightweight. This improves handling and maximizes efficiency. Furthermore, it should be stiff to guarantee low system compliance. To achieve this, an appropriate material such as aluminum should be used and simple design should be chosen.

The brake system is an important part of the wheel assembly and consists of the calliper and disc. Both must be designed to work cohesively with each other, specifically to prevent brake fade.

The brake calliper is the most important component of the braking system as it contains one or more pistons and brake pads. Hydraulic pressure will build up in the piston/s and force the pads against the brake disc, consequently stopping the car. In FSAE racing, the car will travel at high speeds and braking will generate excessive heat quickly. Therefore, it is essential that the brake callipers are lightweight and properly ventilated. Brake callipers must be chosen before the size of the disc, upright and shaft can be evaluated. This decision is based on the size of the wheel and mass of the car.

A floating brake disc is typically used in racing as its overall performance is considerably better than standard brake discs. It reduces the weight of the unsprung mass, dissipates heat quickly due to its large contact surface and at high speeds it won't vibrate. All brakes have an operating temperature range before the mechanisms fail, so it's important to choose the right type of calliper for the function and prevent excessive heat.

The goal is to design the wheel assembly for a race car and to show what steps should be considered to achieve it. The process is easy to track and can be useful for other FSAE design teams.

The rest of this paper is organized as follows. Rules and regulations set by FSAE are provided in Section 2 to determine what applies to the wheel assembly. Design and analysis by using computer programs such as SolidWorks and Ansys are proposed in Section 3. Finally, in Section 4, conclusions are presented.

2. Methods

2.1. Constraints

There are several constraints that must be adhered to when designing the wheel assembly – Formula SAE (FSAE) rules [1], Australian Standards [2] and other constraints. The rules for the FSAE competition act as a constraint on the design of the wheel assembly. All designs must conform to the specified requirements to be eligible for competition, see Table 1.

As the wheel assembly is being designed in parallel with several

* Corresponding author.
E-mail address: greg.wheatley@jcu.edu.au (G. Wheatley).

https://doi.org/10.1016/j.rineng.2021.100244
Received 18 May 2021; Accepted 29 June 2021
Available online 8 July 2021

Table 1
Related rules and constraints.

	Name	Description
FSAE rules [1]	T6.1.2	all A-arm and steering connection points are visible
	T6.5.2	the steering will be placed on the front uprights and must ensure the tyres do not come into contact with the suspension, body or frame
	T11.1 and T11.2	use 8.8 class bolts or higher; fasteners will also be in double shear
	T7.1	The braking system acts on all four wheels where the brake assembly is attached to the front wheel assembly. The rear drive shaft will hold the brake assembly to brake the rear wheels.
Australian Standards [2]	AS1403-2003	Design of Rotating Steel Shafts
	AS2729	Rolling Bearings
	AS1654.1	System of Limits and Fits – Part 1: Bases of Tolerances, Deviations and Fits
	AS1110.1	Bolts
	AS1420	ISO Metric Hexagon Socket Head Cap Screws
	AS4100	Steel Structures
	AS1554	Steel Welds
	AS1664	Aluminum Structures
	AS1665	Aluminum Welds

other components of the car, the design groups in charge of these of components had to be conferred with to determine the method of approach. These discussions resulted in the following design constraints:

- Since the wheel assembly team needs to design steering pickup points the overall geometry of the car comes into consideration. The general idea and approach in FSAE is to keep the wheel base as small as possible. Because of this it was decided early that the steering pick up point would need to be on the front of the upright to give as much room as possible for the engine and cockpit.
- The suspension team and the wheel assembly team need to work closely since both designs constrain each other. The wheel assembly needs to give the suspension team constraints relating to pick up points for the suspension, how far apart and how much offset can be from the axles. The suspension team constrains the design for the wheel assembly since they will need to specify angles and attachments for the A-arms.
- The wheel assembly has also had consultations with the rear drive assembly to assess the best position for brake discs and the type of joins for the rear axle. So far the teams have decided that the brakes will be incorporated into the rear drive assembly.
- The torque from the motor will affect the analysis of the rear hub shaft assembly and these forces will be gathered from both the engine teams and rear drive teams results.

2.2. Design

The design consisted of a shaft with a hub welded to the end and a brake disc mount attached part way down the shaft. The bearing housing then slid on the shaft and butted up against the brake disc mount. Welded steel brackets, shown in Fig. 1, were designed to attach the A-arms to the upright and a steering mounting point was cut into the upright.

The brake calliper mount was a separate piece of a thin suitable aluminum that was welded onto the main upright (see Fig. 2). This would reduce weight and decrease the overall length of the assembly by allowing the calliper to be mounted effectively anywhere along the upright. The main constraint to the overall length of the assembly was the brake calliper. The geometry of the calliper determined how close the brake disc could be to the wheel and in turn how close the entire assembly could be to the hub. Through research many callipers were investigated and the Willwood GP320 [3] was the most suitable for the task due to weight and dimensions (see Fig. 3).

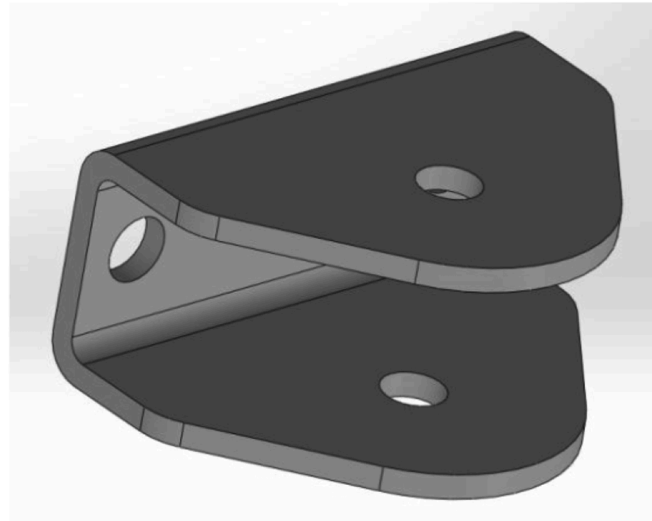

Fig. 1. SolidWorks model of bracket.

The brake mount was designed as a brake hat, see Fig. 4, such that it could be mounted easily over the wheel lugs and also allow the first wheel bearing to be as close to the hub as possible (see Fig. 5).

The brake rotor size was considered to be large enough for two reasons. Firstly, to let the calliper sit over the thickness of the hub plate, decreasing the length of the assembly. And secondly to increase braking performance and cooling. The rotor is made from tempered 5 mm steel with drilled holes for cooling and grit removal. The rotor also has cut outs around the inner radius to reduce heat transfer to the rest of the assembly.

The upright was profile cut from aluminum and welded to the outside of the bearing housing. The whole thickness of the upright was extruded out in the design to accommodate the brake calliper.

2.3. Loading condition

2.3.1. Bolt loads

Through research it was determined that the maximum accelerations the car would experience are 1.5g in braking, before the tyres would lose traction, and 1.7g in cornering. It was noted that the car would not likely experience both the full accelerations at the same time and would more likely experience a portion of the two. Through traction circle calculations, the ‘critical corner’ accelerations were produced.

A simplistic free body diagram (FBD) of the car was used in Engineering Equation Solver (EES). This tool works step by step between points of interest to systematically solve for forces in all directions on the bolts of all four wheels simultaneously. The tool takes inputs as the accelerations on the center of mass and geometry. It then outputs forces in all directions at every point. It was noted that the front bolts oppose the braking force and that the top bolt will carry all of the vertical load due to the pull rod suspension. As shown in Fig. 6, the car was modelled with a wheel base of 1530 mm, a front track of 1200 mm and a rear track of 900 mm. The mass of the car for the analysis was 400 kg and the center of mass was approximated at 350 mm off the ground. Bolt loads are listed in Table 2.

The brake system consists of a brake rotor hat that sits over the hub shaft on which the brake disc is mounted. The brake disc mounting method was chosen to be floating, which is common practice in FSAE. It is also recommended since the disc float reduces heat transfer and helps with small misalignments.

The floating disc is attached with circliped buttons that align semicircle cut outs in the mount and rotor. These buttons transfer the torque to the brake rotor hat and in turn to the hub. With the brake disc

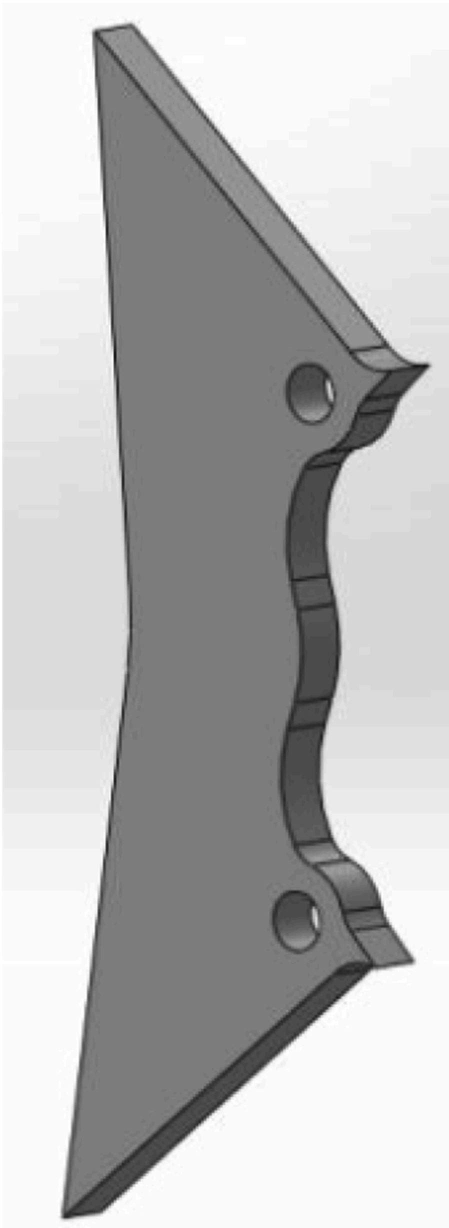

Fig. 2. SolidWorks model of the brake calliper mount.

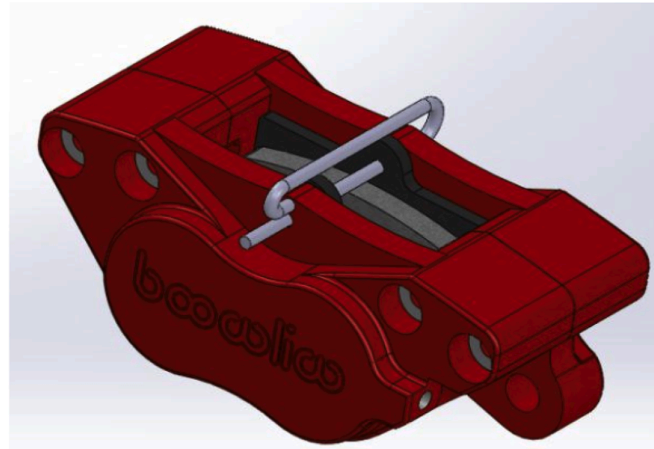

Fig. 3. SolidWorks model of Willwood GP320.

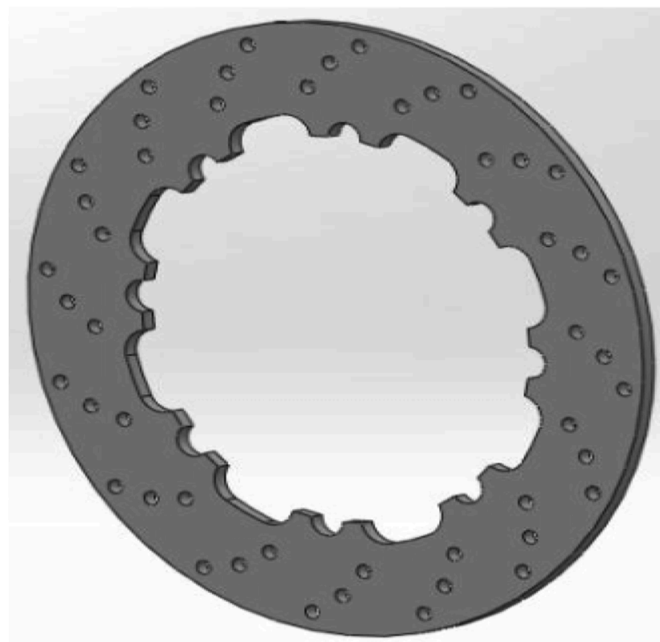

Fig. 4. SolidWorks model of the brake rotor.

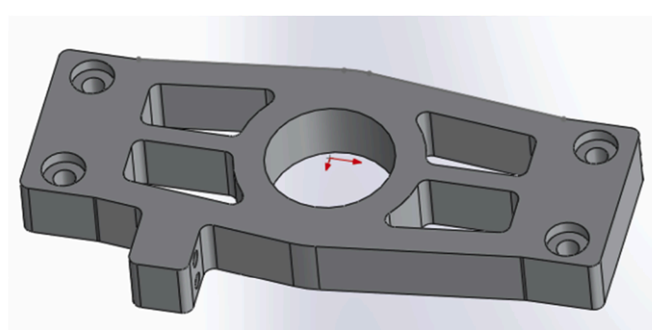

Fig. 5. SolidWorks model of upright.

mounted in this manner, there is no torque applied to the front hub shaft which is a huge advantage.

The brake calliper is mounted on the upright via a welded on aluminum bracket. Under braking the calliper transfers the torque from the slowing wheel to the upright and in turn to the suspension attachment points. These loads are taken into consideration within the load case tool.

The brake rotor hat will be analyzed separate of the rest of the system to increase accuracy and efficiency during analysis. The maximum brake forces are calculated from assuming that the front brakes will need to stop 100% of the car. Since brakes are a safety feature, all assumptions will be conservative. The maximum brake torque was calculated to be about 750Nm.

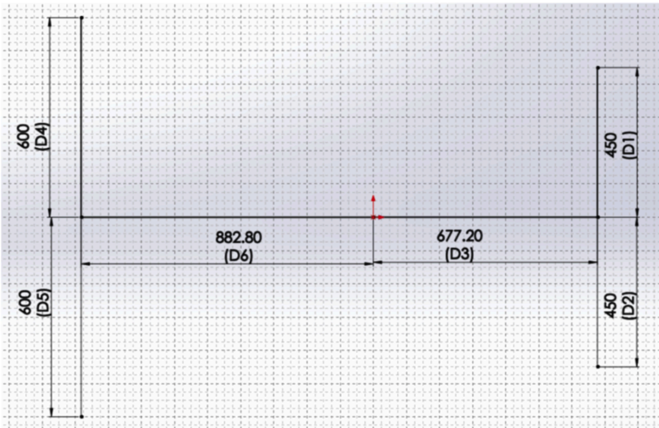

Fig. 6. Dimensions of contact patches relative to the approximated center of mass.

Table 2
Force on bolts of the critical wheel using the load case tool.

	Direction	Maximum braking (N)	Maximum cornering (N)	Critical cornering (N)
Top bolts	X	1225	0	611.8
	Y	−1512	−1825	−2026
	Z	0	−781.9	−623.2
Rear bolts	X	−3493	0	−1745
	Y	0	0	0
	Z	0	2230	−1777

3. Results and discussion

3.1. Brake rotor hat

The brake rotor hat was analyzed in Ansys with a moment applied at the brake button mounts and was fixed at the wheel lug holes. This was a conservative analysis since the friction between the hat and the hub would carry most of the load. The analysis was done at 100 °C as an approximation of the heat it would normally carry.

The initial design consisted of a 6 mm mount plate (constrained for floating system), a 5.4 mm thick pipe section and a 6 mm face plate. The static structural setup in Ansys is shown below in Figs. 7 and 8.

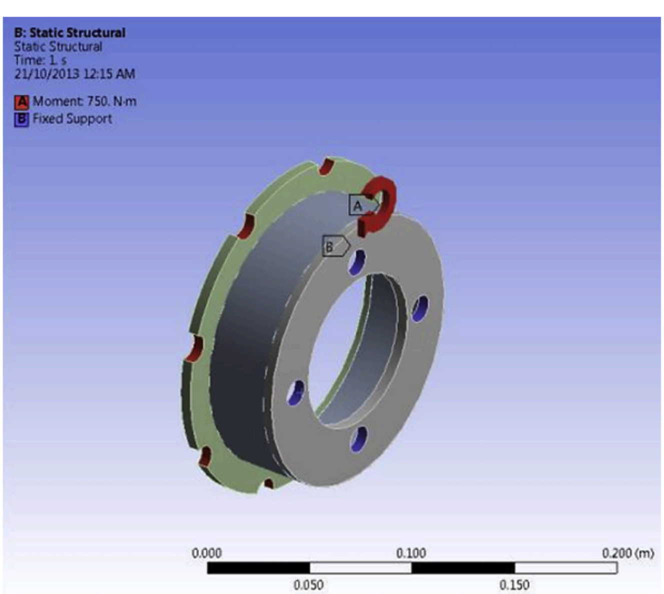

Fig. 7. Load and support setup in Ansys for brake rotor hat.

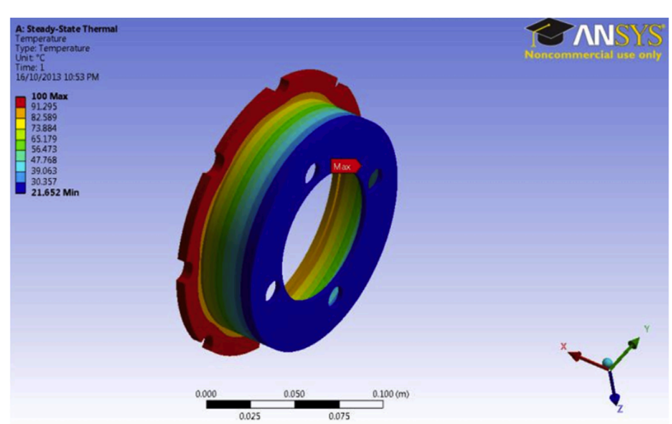

Fig. 8. Temperature plot of the brake rotor hat.

The first analysis set was of the initial design with a 6 mm hub plate and 5.4 mm thick pipe section, the stress contour plot is shown in Fig. 9.

The fatigue analysis for the brake rotor hat was evaluated with a fatigue strength factor of 0.619. The loading was set as zero based under the Goodman stress theory. This was used for all fatigue analysis of the brake rotor hat. The safety factor results is shown in Fig. 10.

It was observed that the safety factor was well above 1 for the majority of the pipe section. The safety factor at the join between the hub plate and the pipe section was just above 1. Due to the welding of the join on the inside, the stress in the area will be reduced considerably.

With these results, the pipe section was reduced to a thickness of 3 mm and the safety factor of the whole assembly was then 1. Furthermore, the next design step was to reduce the thickness of the hub plate to 3 mm. Form Figs. 11 and 12, the brake rotor hat will not fail under maximum load or fatigue and has a safety factor of 1.27. The maximum stress is still expected to decrease in the critical zones due to the added weld in that area to distribute the load.

3.2. Suspension bracket analysis

There are eight brackets in total on the car and two per upright. The load case tool developed in Engineering Equation solver (EES) was used to determine the forces applied to the bolts of the suspension and these forces were applied to the bolt holes on the brackets.

The top and bottom brackets were designed with 4 mm thick steel for different loading cases. From the results showed in Table 3, under all the load cases, the top bracket failed in fatigue along the bend in the material. This problem was solved by welding gussets on either side of a lengthened bracket to support the area that was failing under fatigue, as shown in Fig. 13. On the other hand, the bottom bracket had an acceptable performance without failure.

3.3. Upright

Because of the complex geometry of the assembly, it was analyzed as a whole. This limited the mesh density and the solution time of the model but it was the most accurate way of determine the loads on all the bodies.

With the right contact definitions it was possible to also analyze the forces from the brake calliper at the same time which gave a more accurate analysis. Fig. 14 shows a force and support setup. For the different load cases, only the loads at the brackets were altered using the load case tool developed in EES.

The upright design did not change in concept but did change shape drastically from the preliminary design. The final upright profile cut is out of 32 mm 6061 T6 aluminum alloy and has various weight saving cut outs within its body. There is a large hole 63.5 mm in diameter to suit the

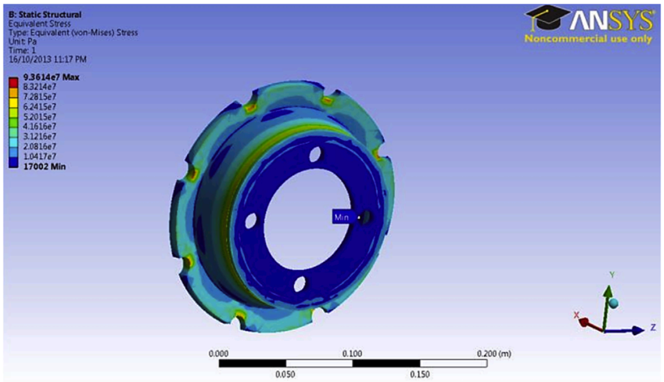

Fig. 9. Stress contour plot of brake rotor hat with 6 mm hub plate and 5.4 mm thick pipe section.

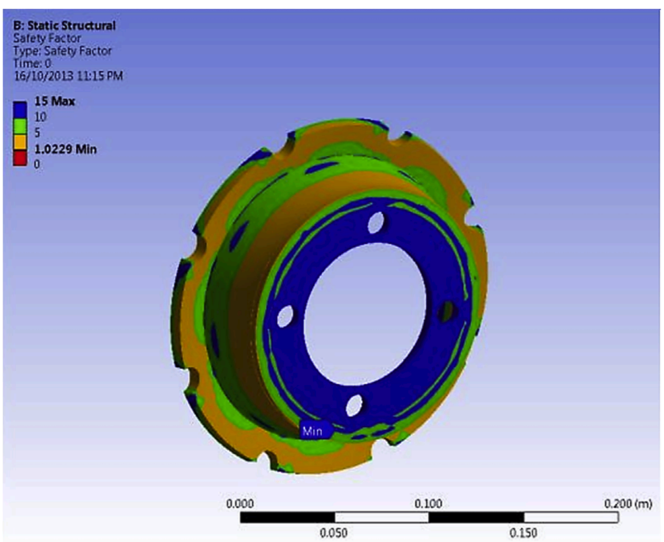

Fig. 10. Safety factor plot of brake rotor hat with 6 mm hub plate.

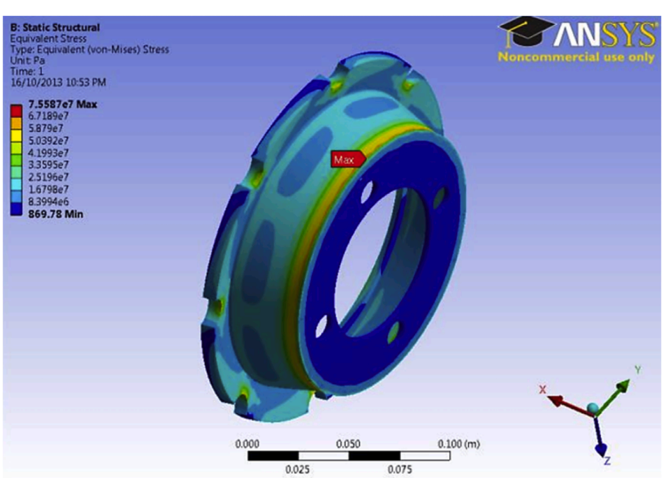

Fig. 11. Stress plot for the brake rotor hat with 3 mm hub plate and 3 mm thick pipe section.

bearing housing and countersunk holes at both bracket mounting points. The stress contour plot can be produced for the critical cornering load case, see Fig. 15.

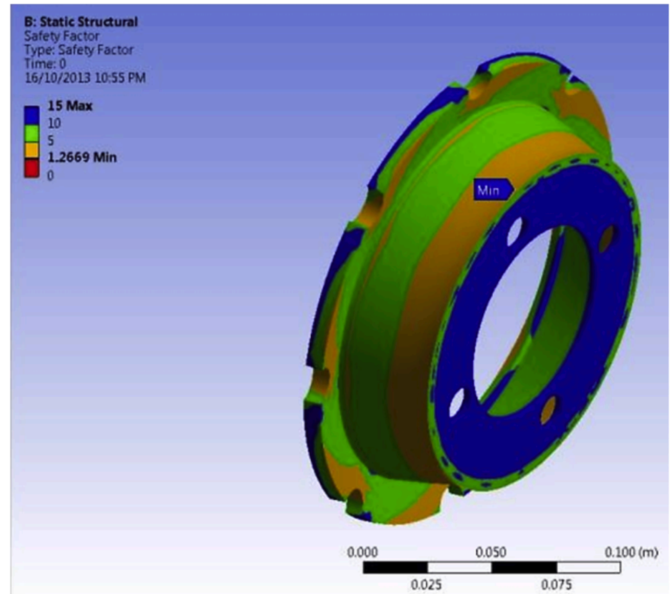

Fig. 12. Safety factor plot for the brake rotor hat with 3 mm hub plate and 3 mm thick pipe section.

Table 3
Safety factors of bracket under different load cases.

Load case	Critical cornering	Maximum cornering	Maximum braking
Top bracket	0.65	0.57	0.7
Bottom bracket	1.93	3.61	1.35

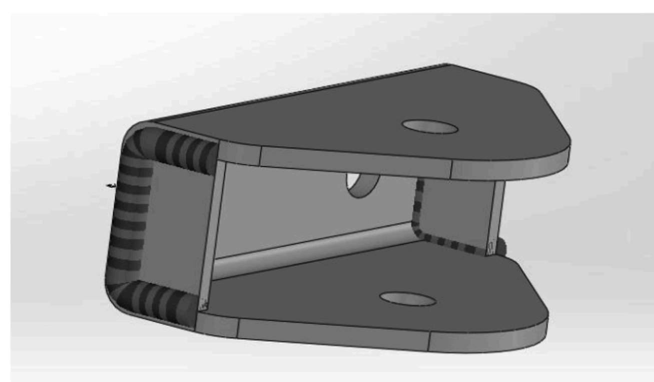

Fig. 13. Design change for top bracket.

Results revealed that the maximum braking load case appears to be most critical on the upright.

The model errors in the bolt holes of the upright have made it difficult to analyze the upright properly. The upright is a body that, from its design, would expect stress concentrations around parts of the complex geometry. Due to the abnormalities it was difficult to analyze such stresses and therefore a conclusion on the life expectancy of the part is hindered. Analysis on the upright needs to be improved with an unlimited amount of nodes or a breakdown of the system, which would require a better understanding of the transfer of forces in the model.

3.4. Bearing housing

The bearing housing was constrained by available size to fit the 30 mm bearing which limited the ability to optimize the bearing housings

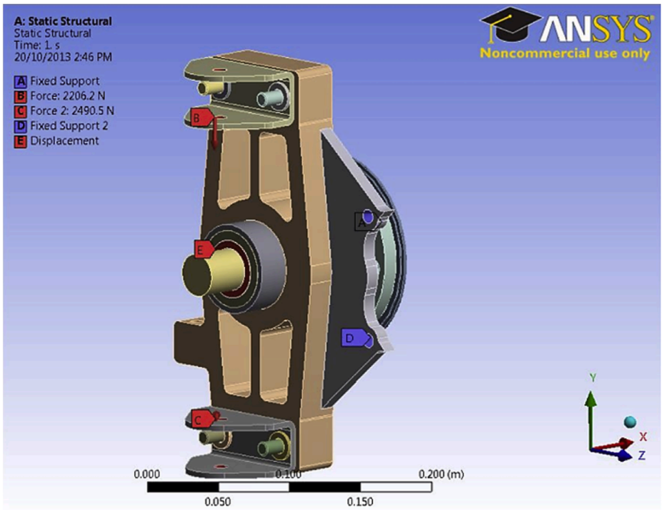

Fig. 14. Load and support setup for assembly analysis.

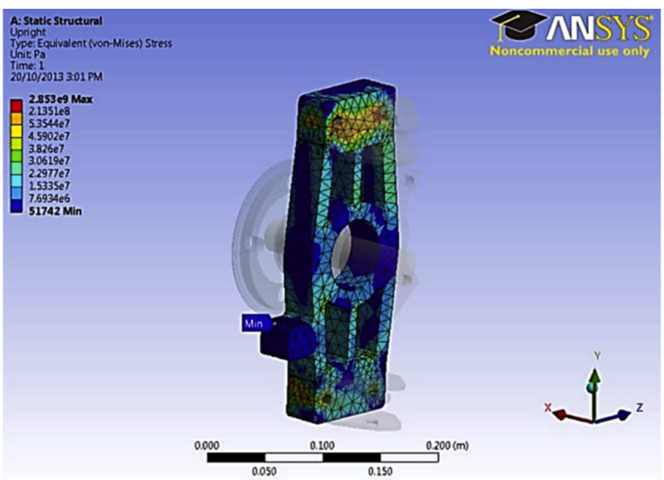

Fig. 15. Stress plot on upright for critical cornering load case.

weight and design. The analysis images below are the worst cases for the bearing housing which was under the critical cornering load case. Figs. 16 and 17 show that under fatigue for the most critical load the proposed bearing housing will have a safety factor of 3.5.

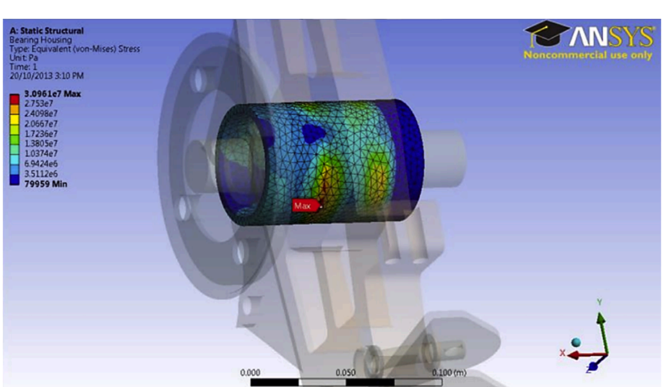

Fig. 16. Stress plot on bearing housing for critical cornering load case.

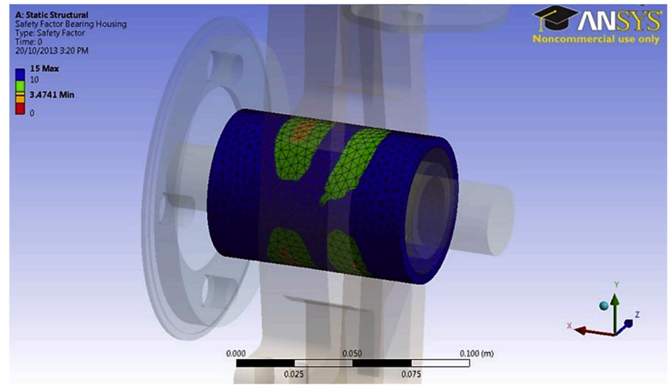

Fig. 17. Safety factor plot on bearing housing for critical cornering load case.

3.5. Hub shaft

The hub shaft was designed as per the Australian Standard AS 1403-2004. The loads on the bearings were calculated for all load cases, and the most conservative values were used to perform fatigue analysis on the shaft. To determine the reaction forces at the bearings, the wheel assembly as a whole was first analyzed. The reaction forces and moments to the load forces were found around the hub faceplate (see below calculations and formula), and then these forces were used to analyze the hub shaft and face plate alone. The reaction forces were then able to be found at the bearings. It was found that shear forces acted on the shaft in both the x and z direction.

The following equations were derived such that the bolt forces (T_x, T_y, T_z, B_x, B_y, B_z) for all load cases could be used to find the resultant forces acting on the hub shaft at the bearings (R_{1x}, R_{1y}, R_{2x}, R_{2y}). The load cases used as inputs are as shown in Table 2. Fig. 18 show the free-body diagrams for system. B, C, D and E are equal to 0.021 m, 0.091 m, 0.118 m and 0.125 m respectively (see Figs. 19–21).

Forces on entire assembly are as follows:

$$\sum F_x = 0 \rightarrow R_{wx} = -(T_x + B_x) \tag{1}$$

$$\sum F_y = 0 \rightarrow R_{wy} = -W \tag{2}$$

$$\sum F_z = 0 \rightarrow R_{wz} = -(T_z + B_z) \tag{3}$$

$$\sum M_x = 0 \rightarrow M_{wx} = E(T_z - B_z) + WC \tag{4}$$

$$\sum M_y = 0 \rightarrow M_{xy} = C(T_x + B_x) \tag{5}$$

And Forces on hub shaft

$$\sum F_x = 0 \rightarrow R_{1x} + R_{2x} + R_{wx} = 0 \tag{6}$$

$$\sum F_y = 0 \rightarrow R_{1y} + R_{2y} + R_{wy} = 0 \tag{7}$$

$$\sum M_x = 0 \rightarrow -R_{1y}C - R_{2y}B + M_{wx} = 0 \xrightarrow{(6)} R_{2y} = \frac{R_{wy} + M_{wx}}{B - C} \tag{8}$$

$$\sum M_x = 0 \rightarrow -R_{1x}C - R_{2x}B + M_{wy} = 0 \xrightarrow{(7)} R_{2x} = \frac{R_{wx} + M_{wy}}{B - C} \tag{9}$$

Bending moment can be defined as

$$M_q = R_{1y}\,(C - B) \tag{10}$$

From the Australian Standard AS 1403-2004, Equivalent torque and minimum shaft diameter:

$$T_E = 1.15\sqrt{M_q^2 + 075T_q^2} \tag{11}$$

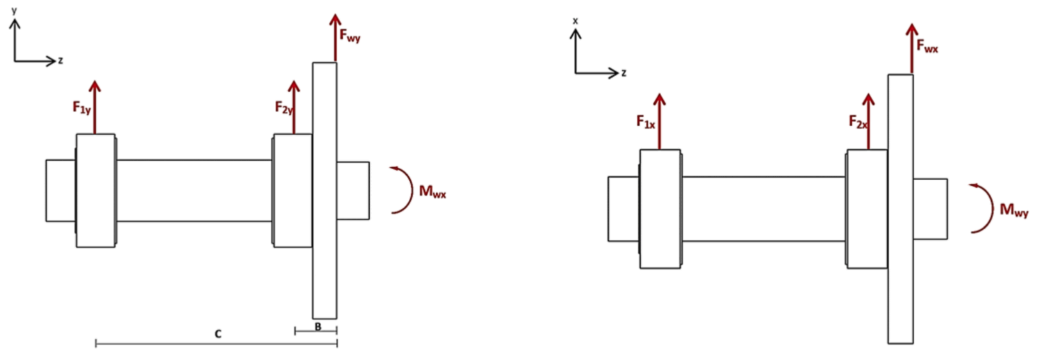

(a)

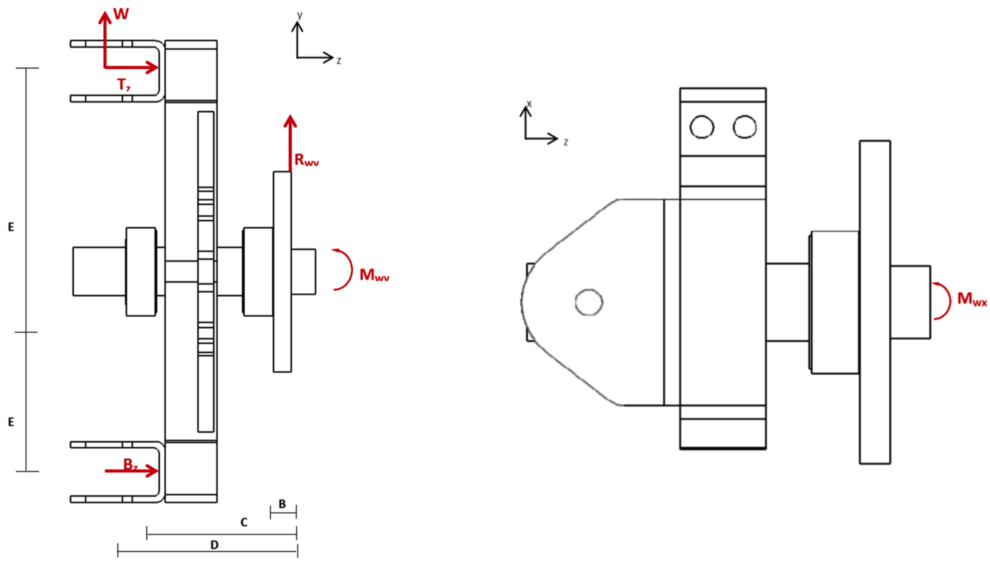

(b)

Fig. 18. Free body diagram of (a) Shaft and (b) Assembly.

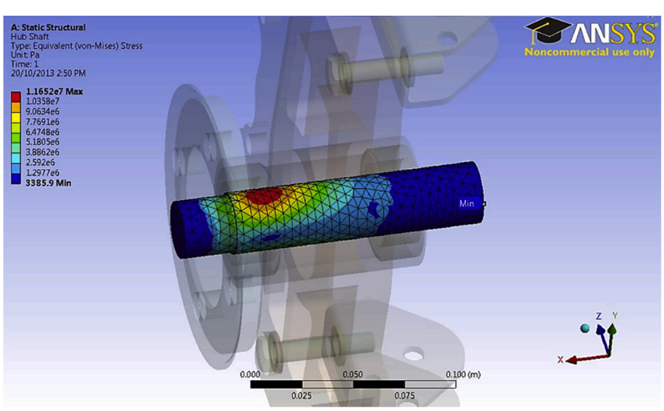

Fig. 19. Equivalent stress of hub shaft under critical load.

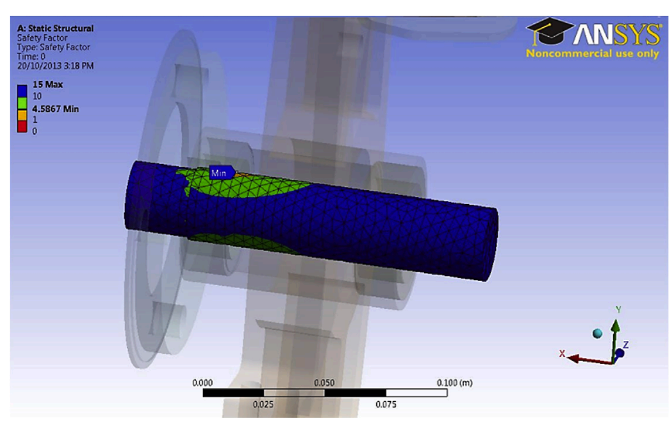

Fig. 20. Safety factor for critical load case.

For the front hub shafts, the maximum actual torque, T_q, is zero, as there are no engine forces and brake forces are applied directly to the wheel

$$T_E = 1.15\ M_q \tag{12}$$

The following equation is used for calculating the minimum diameter of the shaft for the case where the number of mechanism starts per year is less than 600, and the number of revolutions of the shaft per year is greater than 900.

$$D^3 = \frac{10^4 F_s}{F_R}\sqrt{\left[K_s K\left(M_q + \frac{P_q D}{8000}\right)\right]^2 + \frac{3}{4}T_q^2} \tag{13}$$

This was considered reasonable, as the number of revolutions will be much greater than 900 per year, but the number of vehicle starts is predicted to be less than 600. More conservative formulae were

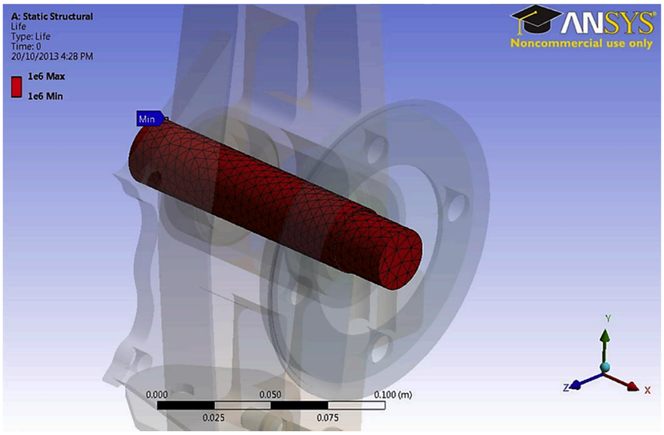

Fig. 21. Fatigue life for critical load case.

described in the AS 1403- 2004, but the biggest factor altered in these formulae was the torque term. As the torque present in the front hub shaft is zero, the more conservative formulae were considered unnecessary.

The axial force, P_q, was considered negligible for the front hub shaft, as all axial forces created by reactions in the wheel for critical load cases will be resisted by the bearings.

$$D^3 = \frac{10^4 F_s}{F_R} \sqrt{\left[K_s K\left(M_q + \frac{P_q D}{8000}\right)\right]^2 + \frac{3}{4}T_q^2} \tag{14}$$

The values of the endurance limit, F_R, size factor, K_s, and stress raising factor, K, were found from the relevant tables and sections in the Australian Standard. The primary stress raising factor was the transition fit of the bearings on the shaft.

Table 4 shows the parameters of the system. The values which produced the more conservative values were used to calculate the equivalent torque.

The most conservative equivalent torque and bending moment were found to be for the maximum cornering case. These values were used for the hub shaft diameter equations. The hub shaft was analyzed using FEA using a diameter of 30 mm, 150 in length and it is made from AIS 1040 steel round. In the most critical load cases; the critical load case and the maximum cornering load case; the diameter was found to have a safety factor higher than 1.2, as seen in the Figures below.

The decision to use AIS 1040 steel for the hub shafts was based on the material properties shown in Table 5, which shows a comparison of most common steels. 1045 steel is more readily welded than higher-carbon steel such as 4340 and 4140, while retaining its tensile strength after welding, unlike 1214 steel. It has a higher tensile strength than 1020, 1030, and 1045 steels.

The bearings were decided by the hub shaft diameter and the appropriate type. It was noted that sealed tapered bearings would be suitable and easy to maintain. The bearing housing relied heavily on the bearing size and the available pipe dimensions. The material also needed to be weldable to the material of the upright. With the 30 mm bearing the most suitable bearing housing tube was a 63.5 O.D. 6061 T6 6.35 mm thick tube. This would need to be machined out slightly for the housing bearings to sit in the recommended fit.

Table 5
Material properties of different steels [4].

Steel	S_{ut} (MPa)	S_y (MPa)	ρ (Kg. m^3)	Welding Properties
1020	448.2	330.9	7861	Readily Weldable – MIG or TIG
1030 (As Rolled)	551.6	344.7	7850	Weldable by all methods. For heavy sections, advised to
1040	620.5	330.9	7845	Weldable by all methods. Can be pre-heated (149–260 C)
1045	600	300	7870	Readily welded in cold drawn or turned and polished
1214	400	290		Not weldable without reduction in tensile strength. Not
4140 (Normalised)	1020.4	655	7850	Should be welded in hardened and tempered condition.
4140 (Annealed)	655	417.1	7850	As above.
4340 (Normalised)	1279	861.8	7750	Welding in hardened and tempered condition not
4340 (Annealed)	744.6	472.3	7750	As above.

4. Conclusions

This paper provides the design process of wheel assembly for a race car. To ensure the quality, the proposed system is designed based on the FSAE rules and Australian standards. The justification is achieved through finite element analysis by investigating the stress distribution and the safety factor of each part of the system including the upright, braking system and hub shaft. The final upright is out of 32 mm 6061 T6 aluminum alloy with a large hole 63.5 mm in diameter. Although the analysis wasn't conclusive, it still appeared that the upright was strong enough when neglecting the abnormalities. It was decided that with the 30 mm bearing the most suitable bearing housing tube was a 63.5 O.D. 6061 T6 6.35 mm thick tube. The hub shaft is 150 in length and made from AIS 1040 steel round, 30 mm in diameter. The final brake rotor hat consists of a 3 mm hub plate that fits over the lugs, a 3 mm thick pipe section to offset the rotor and a 6 mm mounting plate to mount the floating rotor. The final brake rotor hat consists of a 3 mm hub plate that fits over the lugs, a 3 mm thick pipe section to offset the rotor and a 6 mm mounting plate to mount the floating rotor.

Credit author statement

G. Wheatley: Methodology, Validation, Writing - original draft, Formal analysis. M. Zaeimi: Writing - review & editing.

Ethics statement

Not applicable.

Funding

This research did not receive any specific grant from funding agencies in the public, commercial, or not-for-profit sectors.

Table 4
Reaction forces and bending moments (Mq) at bearings for each load case.

Load case	R_{b1y} (N)	R_{b2y} (N)	R_{b1x} (N)	R_{b2x}(N)	M_q(y) (Nm)	M_q(x) (Nm)	M_q (max) (Nm)	T_e(Nm)
Critical corner with 1g bump	−8777.8	5899.8	1993.6	−2946.4	−570.6	129.6	570.6	656.1
Max corner	−11030.9	8623.9	0	0	−717.0	0	717.0	824.6
Max brake	−2186.6	674.6	4745.4	−7013.4	−142.1	308.4	308.4	354.7
Critical corner	−7545.7	5519.7	2371.0	−3504.2	−490.5	154.1	490.5	564.0

Declaration of competing interest

The authors declare that they have no known competing financial interests or personal relationships that could have appeared to influence the work reported in this paper.

Acknowledgments

Not applicable.

References

[1] Available:, Formula SAE Rules, 2018 https://www.fsaeonline.com/content/2017-18%20FSAE%20Rules%209.2.16a.pdf.
[2] SAI GLOBAL, Available, https://saiglobalgroup.com.
[3] GP320 Calliper, Available at: https://www.wilwood.com/calipers/CaliperList?subname=GP320.
[4] SAE steels, Available at: https://weldreality.com/HYSteels.htm.